Title
Spectral breadth and laminar distribution of thalamocortical inputs to A1

Journal
Journal of Neurophysiology, 115(4)

ISSN
0022-3077

Authors
Intskirveli, Irakli
Joshi, Anar
Vizcarra-Chacón, Bianca Julieta
et al.

Publication Date
2016-04-01

DOI
10.1152/jn.00887.2015

J Neurophysiol 115: 2083–2094, 2016.
First published February 17, 2016; doi:10.1152/jn.00887.2015.

CALL FOR PAPERS | *Auditory System Plasticity*

Spectral breadth and laminar distribution of thalamocortical inputs to A1

Irakli Intskirveli, Anar Joshi, Bianca Julieta Vizcarra-Chacón, and Raju Metherate
Department of Neurobiology and Behavior and Center for Hearing Research, University of California, Irvine, California

Submitted 15 September 2015; accepted in final form 15 February 2016

Intskirveli I, Joshi A, Vizcarra-Chacón BJ, Metherate R. Spectral breadth and laminar distribution of thalamocortical inputs to A1. *J Neurophysiol* 115: 2083–2094, 2016. First published February 17, 2016; doi:10.1152/jn.00887.2015.—The GABAergic agonist muscimol is used to inactivate brain regions in order to reveal afferent inputs in isolation. However, muscimol's use in primary auditory cortex (A1) has been questioned on the grounds that it may unintentionally suppress thalamocortical inputs. We tested whether muscimol can preferentially suppress cortical, but not thalamocortical, circuits in urethane-anesthetized mice. We recorded tone-evoked current source density profiles to determine frequency receptive fields (RFs) for three current sinks: the "layer 4" sink (fastest onset, middle-layer sink) and current sinks 100 μm above ("layer 2/3") and 300 μm below ("layer 5/6") the main input. We first determined effects of muscimol dose (0.01–1 mM) on the characteristic frequency (CF) tone-evoked layer 4 sink. An "ideal" dose (100 μM) had no effect on CF-evoked sink onset latency or initial response but reduced peak amplitude by >80%, implying inhibition of intracortical, but not thalamocortical, activity. We extended the analysis to current sinks in layers 2/3 and 5/6 and for all three sinks determined RF breadth (quarter-octave steps, 20 dB above CF threshold). Muscimol reduced RF breadth 42% in layer 2/3 (from 2.4 ± 0.14 to 1.4 ± 0.11 octaves), 14% in layer 4 (2.2 ± 0.12 to 1.9 ± 0.10 octaves), and not at all in layer 5/6 (1.8 ± 0.10 to 1.7 ± 0.12 octaves). The results provide an estimate of the laminar and spectral extent of thalamocortical projections and support the hypothesis that intracortical pathways contribute to spectral integration in A1.

auditory cortex; muscimol; mouse; current source density; thalamocortical input

ONE APPROACH to understanding the function of primary auditory cortex (A1) is to determine the extent to which neural activity in A1 reflects processing within the cortex. For spectral integration in A1, an important question is the extent to which frequency receptive fields (RFs) reflect intracortical processing as opposed to subcortical spectral integration that is relayed to A1 (Winer et al. 2005). Extracellular recordings of action potentials (single or multiple units) show that RF breadth remains relatively constant throughout the lemniscal auditory pathway (Calford et al. 1983), suggesting that cortical RFs simply reflect subcortical processing. However, pharmacological manipulations and intracellular recordings demonstrate extensive subthreshold inputs to cortical neurons and suggest that the total spectral input (including subthreshold) to a neuron may be broader in A1 than in subcortical relay stations (Kaur et al. 2004; Metherate 2011b; Palombi and Caspary 1992, 1996; Tan et al. 2004; Wang et al. 2000; Wehr and Zador 2003). One implication of extensive subthreshold RFs is that modulation of such inputs might underlie rapid RF plasticity observed in A1 during behavior and other manipulations (Fritz et al. 2003; Froemke et al. 2007; Weinberger 2004).

The representation of characteristic frequency (CF) in the auditory pathway clearly reflects topographic anatomical projections, whereby the tonotopic representation of frequency established in the cochlea is preserved throughout the lemniscal auditory system, culminating in tonotopic thalamocortical projections to A1 (Hackett et al. 2011; Miller et al. 2001; Winer et al. 2005). As a result, broad spectral integration in A1 could simply involve convergence of multiple thalamocortical projections. Alternatively, or in addition, spectral integration may involve intracortical ("horizontal") pathways that link regions with different CFs. Determining whether and how these circuits contribute to spectral integration is an important step toward understanding neural processing and plasticity in A1.

A useful tool to address locus-of-function questions is the drug muscimol, a GABA-A receptor agonist that is thought to inhibit all neurons and thereby "silence" a region without affecting axons of passage (Edeline et al. 2002; Martin and Ghez 1999). In auditory cortex, muscimol has been used to silence intracortical activity in order to determine the necessity of cortex for specific auditory behaviors (Jaramillo and Zador 2011; Smith et al. 2004; Talwar et al. 2001). In other studies, muscimol is used not just to inhibit neurons but in doing so to isolate and identify afferent inputs. In principle, electrodes at the site of muscimol administration can record monosynaptic afferent inputs, since muscimol-induced inhibition does not prevent synaptic transmission but can reduce the amplitude of excitatory postsynaptic potentials (EPSPs) to prevent action potentials and subsequent intracortical activity. Any afferent-evoked activity should therefore, ideally, reflect monosynaptic inputs and not intracortical circuits. To achieve this ideal effect, muscimol should reduce EPSPs sufficiently to prevent action potentials, but not so much as to preclude detection of the EPSPs themselves (e.g., due to excessive postsynaptic shunting). Studies have used this approach to examine the spectral breadth of inputs to A1, i.e., delivering muscimol into A1 and assuming that remaining acoustic-evoked responses reflect thalamocortical inputs (Happel et al. 2010; Kaur et al. 2004). However, this approach has been questioned on the grounds that muscimol may unintentionally reduce afferent synaptic transmission via nonspecific actions at presynaptic

Address for reprint requests and other correspondence: R. Metherate, Dept. of Neurobiology and Behavior, Univ. of California, Irvine, 2205 McGaugh Hall, Irvine, CA 92697-4550 (e-mail: raju.metherate@uci.edu).

GABA-B receptors (Liu et al. 2007; Yamauchi et al. 2000). Although such nonspecific actions have not been observed in neocortex, several recent studies have silenced cortical neurons with muscimol paired with a second drug to block possible actions on GABA-B receptors (Happel et al. 2010; Hogsden et al. 2011; Liu et al. 2007; Zhou et al. 2010). However, this approach is complicated, in terms of both pharmacology and interpretation (e.g., blockade of presynaptic GABA-B receptors also will affect postsynaptic GABA-B receptors) (see DISCUSSION). Given these difficulties, the present study was undertaken to reexamine whether muscimol can be used alone in order to silence cortical neurons and isolate afferent inputs.

We examine the assumption that muscimol can suppress intracortical transmission while leaving thalamocortical inputs unaffected. The results show that muscimol can act as intended, but only at an appropriate dose. We then use this optimal dose to determine the laminar and spectral extent of thalamocortical inputs to A1 and, by inference, the contribution of intracortical circuits to spectral integration in A1.

MATERIALS AND METHODS

Animal preparation. Adult (60–80 day old) male FVB mice were used for all procedures in accordance with the National Institutes of Health *Guide for the Care and Use of Laboratory Animals* and as approved by the University of California, Irvine Institutional Animal Care and Use Committee. Mice were anesthetized with urethane (0.7 g/kg ip; Sigma) and xylazine (13 mg/kg ip; Phoenix Pharmaceutics), placed in a sound-attenuating chamber (AC-3; IAC Acoustics), and maintained at 37°C. Anesthesia was supplemented as necessary with urethane (0.13 g/kg) and xylazine (1.3 mg/kg) via an intraperitoneal catheter to avoid movement. The head was secured in a stereotaxic frame (model 923; Kopf Instruments) with blunt earbars. After a midline incision, the skull was cleared and secured to a custom head holder. A craniotomy was performed over the right auditory cortex, and the exposed brain was kept moist with warmed saline. After the craniotomy, the blunt earbars were removed to permit acoustic stimulation.

Electrophysiology and acoustic stimulation. Tone-evoked local field potentials (LFPs) were recorded with a glass micropipette filled with 1 M NaCl (~1 MΩ at 1 kHz) for mapping A1 or a 16-channel silicon multiprobe (~2–3 MΩ at 1 kHz for each 177-μm^2 recording site, 100-μm separation between recording sites; NeuroNexus Technologies) for current source densities (CSDs) and were filtered and amplified (1 Hz to 1 kHz, AI-401, CyberAmp 380; Axon Instruments), digitized (Digidata 1322A; Axon Instruments), and stored on a computer (Apple Macintosh running AxoGraph software). Acoustic stimuli were digitally synthesized and controlled with custom software and delivered through an open-field speaker (FF-1 with AS1 driver; Tucker-Davis Technologies) positioned ~3 cm in front of the left ear. For calibration [sound pressure level (SPL), in dB re: 20 μPa] a microphone (model 4939 and Nexus amplifier; Brüel and Kjaer) was positioned in place for the animal at the tip of the left earbar. Tones were 100 ms in duration with 5-ms linear rise and fall ramps (range 5–40 kHz and −10 dB to 70 dB SPL). During data collection, stimuli were delivered at a rate of 0.5/s in sets of 25 trials.

Determination of A1 recording site. To find a recording site in A1, initially we recorded tone-evoked responses from multiple sites ~200–250 μm apart along the anterior-posterior axis in auditory cortex with a micropipette. Based on responses to a standard set of tones (5–40 kHz in 2.5-kHz steps, −10 dB to 70 dB SPL in 5-dB steps), we determined CF (frequency with the lowest threshold) for each recording site. Initial maps of CF were determined from LFP recordings at the cortical surface, with subsequent confirmation at a few sites with multiunit recordings in layer 4 (~400-μm depth). CF maps were constructed to confirm the tonotopy expected for A1, including a reversal of tonotopy at the border with the anterior auditory field (Stiebler et al. 1997). We then chose a site near the middle of the frequency range represented in A1, with a CF of ~20 kHz, so that the RF could be spanned by the 5–40 kHz range of the stimulus generation system, and mapped along the dorsoventral axis of the presumed isofrequency region to find the layer 4 site with the shortest-latency, largest-amplitude LFP. This site was used for all subsequent procedures. We inserted a 16-channel multiprobe perpendicular to the pial surface to record LFPs throughout the cortical depth and more precisely redetermined CF (1-kHz steps) and threshold (5-dB steps) based on the onset latency and initial slope of LFPs recorded 300–400 μm below the surface. Tone-evoked LFPs were considered threshold responses when their amplitude exceeded three times the standard deviation (3 × SD) of the mean baseline determined over the 10 ms preceding the tone.

Drug application. Neural activity was inhibited with the GABA-A receptor agonist muscimol (5-aminomethyl-3-hydroxyisoxazole; Sigma). During each experiment, a stock solution of muscimol (1 mg/ml, 8.7 mM) was diluted in artificial cerebrospinal fluid (ACSF, in mM: 125 NaCl, 2.5 KCl, 25 $NaHCO_3$, 1.25 KH_2PO_4, 1.2 $MgSO_4$, 2.0 $CaCl_2$, 10 dextrose) to the desired concentration.

For surface application, muscimol was applied close to the multiprobe in two steps over 5 min with a 0.5-μl Hamilton syringe. For cortical microinjection, we used a 0.5-μl Hamilton syringe fitted with a micropipette (~20-μm tip); muscimol (or vehicle) was delivered over 5–7 min and the injector left in place for another 5 min before removal. The injected solution also contained 2% tetramethylrhodamine dextran (molecular weight 10,000; Molecular Probes or Invitrogen) or fluorescein dextran (molecular weight 10,000; Molecular Probes) to mark injection sites. Data acquisition in muscimol began after ~20 min and continued for 30–45 min, long enough to repeat RF determination two or three times. For seven animals in which RFs were determined three times—starting approximately 20, 35, and 50 min after muscimol—the suppression of CF-evoked responses in layer 4 did not change over this period, indicating a stable effect of muscimol (*t*-tests with Sidak-Bonferroni correction for multiple comparisons; P values > 0.05).

Data analysis. Each recorded tone-evoked response is the average response to 25 stimuli. CSD profiles were constructed off-line as described previously (Intskirveli and Metherate 2012). One-dimensional CSD profiles are the second spatial derivative of the LFP laminar profile (Muller-Preuss and Mitzdorf 1984); conventionally, a current sink implies the location, timing, and magnitude of underlying synaptic excitation. The response onset was defined as the time at which the CSD trace crossed a threshold 3 × SD above baseline. Multiunit activity (MUA) was extracted from single-trial, tone-evoked LFPs in layer 4 with a high-pass filter (>500 Hz), rectified, and averaged across sets of 25 trials (O'Connell et al. 2011). Acoustic-evoked MUA was quantified by measuring the response amplitude from 20 to 50 ms from onset; the earliest response was avoided to minimize effects of LFP leakage through the filter. All mean data are reported ±SE except where as noted for SD of LFP spontaneous fluctuations. Statistical comparisons were performed with Microsoft Excel or JMP. Tests of related means (pre- vs. postdrug) were paired *t*-tests (2 tailed). Tests of independent means were *t*-test or ANOVA ($\alpha = 0.05$).

RESULTS

We located A1 by microelectrode mapping in urethane-xylazine-anesthetized adult mice ($n = 22$) and then inserted a 16-channel multiprobe into the cortex at a site with CF of ~20 kHz (mean CF 20.2 ± 0.62 kHz), near the middle of the tonotopic representation in A1, so that RFs could be determined as fully as possible in quarter-octave steps up to ~1 octave above CF and ~2 octaves below (within the 5–40 kHz

range of the stimulation system). The multiprobe was aligned perpendicular to the cortical layers, with recording sites spaced 100 μm apart so that recordings spanned all six layers (overall A1 thickness ~1 mm). Although stimulus intensity was varied during the experiment, e.g., to determine CF, all results presented here were obtained 20 dB above CF threshold, except for data on CF threshold itself.

CF-evoked CSD profile. Figure 1 shows a typical CF tone-evoked response in A1. CF-evoked LFPs (Fig. 1*A*, *left*) were acquired and converted off-line to CSD traces and interpolated color plots (Fig. 1*A*, *center* and *right*). The most reliable current sinks are depicted as red traces in Fig. 1*A*, *center*: the shortest-latency sink in the middle layers was recorded at a depth of either 400 μm (as in Fig. 1*A*) or 300 μm, and is referred to as the "layer 4" current sink since it likely reflects the main thalamocortical input. A second current sink occurred 100 μm above the layer 4 sink and is referred to as the "layer 2/3" current sink. Note that the onset of the layer 2/3 response actually is a very brief current source (negative-polarity transient of a few milliseconds duration) that coincides with the onset of the layer 4 sink, suggesting that the initial thalamocortical current sink in layer 4 is associated with a current source in layer 2/3 (for a higher-resolution example of this consistent finding, see traces in Fig. 5*A*). In most (~80%) cases, a third current sink occurred 300 μm below layer 4 and is referred to as the "layer 5/6" current sink. As in Fig. 1*A*, the current sinks in layers 2/3 and 4 typically merged for the duration of the 100-ms stimulus, whereas the layer 5/6 sink was isolated and brief, ~20–30 ms in duration.

The three current sinks differed in onset latency, as shown in Fig. 1*B* for all animals. The layer 4 sink had an onset latency of 16.5 ± 0.78 ms (n = 22), which is shorter than that of the layer 2/3 sink (20.5 ± 1.88 ms; paired t-test, P = 0.029) and longer than that of the layer 5/6 sink (13.1 ± 1.57 ms, $P <$ 0.001). The laminar location, latency, and duration of the layer 5/6 current sink suggest that it results from a collateral of the main thalamocortical projection to layer 4, as noted previously (Cruikshank et al. 2002; Romanski and LeDoux 1993; Zhou et al. 2010), and the difference in onset latencies over a distance of 300 μm implies a conduction velocity of ~0.1 m/s, consistent with intracortical (unmyelinated axon) velocities (Salami et al. 2003). The onset latency of the layer 2/3 sink is considerably longer than expected for a monosynaptic input, since a similar conduction velocity over the additional 100-μm distance from layer 4 should add only ~1 ms to the latency (instead of the observed ~4 ms). Thus the three current sinks in layers 2/3, 4, and 5/6 appear to reflect distinct (though interdependent) synaptic responses, and are the focus of RESULTS.

Muscimol's dose-dependent suppression of CF-evoked response. We microapplied muscimol to the A1 region adjacent to the multiprobe, either onto the cortical surface (0.5-μl volume delivered over 5 min) or into the middle layers (~400-μm depth, 0.05- to 0.1-μl volume delivered over 5–7 min), using a range of concentrations from 10 μM to 1 mM (1 dose per animal). Results from the two application methods were similar and are combined, except when explicitly compared (e.g., Fig. 4*B*).

To assess muscimol's inhibition of cortical neurons independently of its effect on tone-evoked responses, we measured its effect on spontaneous LFP fluctuations. Spontaneous LFPs—a local measure of the cortical EEG—appear to reflect membrane potential fluctuations that are synchronized among neurons (Metherate et al. 1992; Steriade et al. 1993), and as such should be reduced by inhibition of cortical neurons. We quantified these fluctuations as the SD of the spontaneous LFP

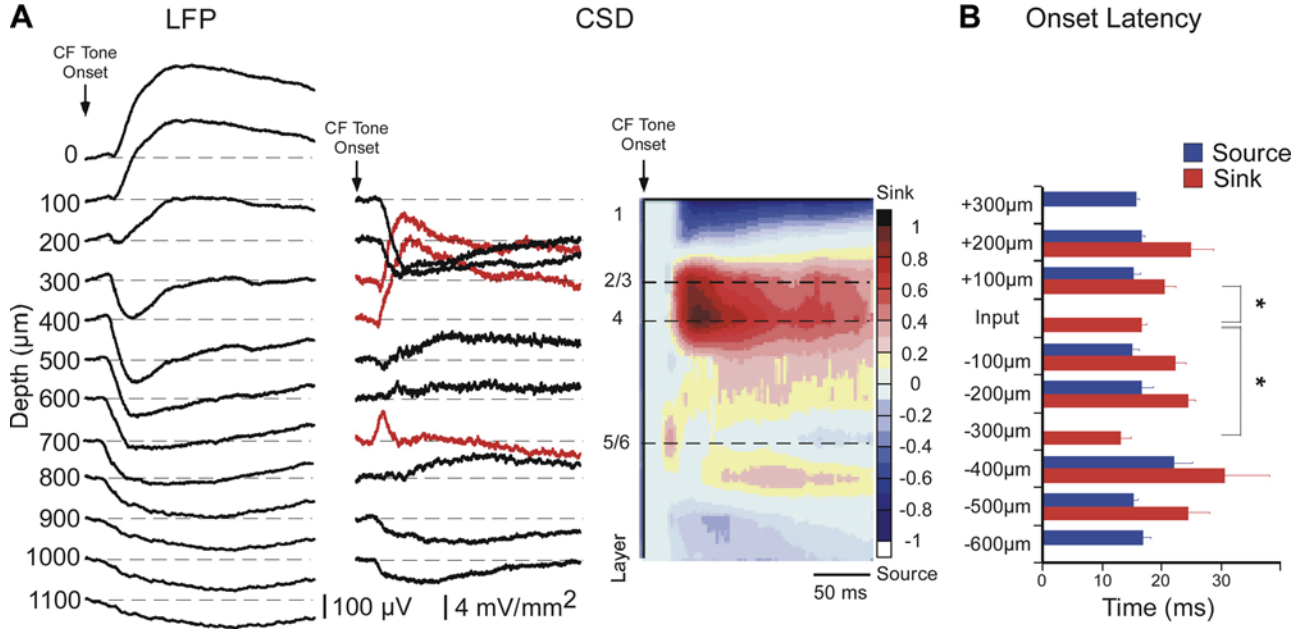

Fig. 1. Characteristic frequency (CF)-evoked current source density (CSD) profile exhibits 3 short-latency current sinks. *A*: example of tone-evoked local field potentials (LFPs) recorded from 12 channels of the multiprobe (*left*; 100 μm between channels) and derived CSD traces (*center*, current sinks are positive polarity). Red traces indicate the 3 current sinks that are the focus of this study. CSD traces are normalized to peak amplitudes and interpolated to produce CSD color plot (*right*). Numbers to *left* of color plot indicate the approximate location of cortical layers based on the earliest middle-layer sink (designated as Input, or layer 4). *B*: mean onset latency of first sink and source at each recording site relative to the Input layer, for all animals (n = 22). Onset of sink or source defined as first positive or negative deflection, respectively, in each CSD trace. Onset latencies among the 3 main current sinks were compared (*; see RESULTS).

during the 100-ms interval preceding each stimulus; responses were averaged in groups of 25 trials (2-s intertrial interval). Figure 2*A* shows an example of spontaneous LFPs in layer 4 with twenty-five 100-ms epochs overlaid, before and after muscimol. The SD was normalized to its predrug value, which across animals was reduced ~50% by muscimol (100 μM dose, Fig. 2*A* histogram; postmuscimol SD is 0.56 ± 0.075 of predrug value; paired *t*-test, $n = 9$, $P = 0.002$). A similar measure of muscimol's effect in layer 4 was obtained for each animal and averaged across animals for each drug concentration. Group data are in Fig. 2*A*, *bottom*. At the lowest concentrations (10–50 μM) muscimol had no effect on LFP fluctuations (1.02 ± 0.080 of predrug value; paired *t*-test, $n = 4$, $P > 0.05$), but 100 μM muscimol reduced the SD ~40% (0.59 ± 0.046, $n = 9$, *t*-test, $P < 0.001$). These data indicate that muscimol inhibits spontaneous LFP fluctuations in a dose-dependent manner.

Next we examined the effects of muscimol on acoustic-evoked responses. To determine whether muscimol inhibits intracortical activity without affecting thalamocortical inputs, we focused on the CF-evoked current sink in layer 4 as it is the most easily interpreted: the earliest portion of the current sink undoubtedly reflects monosynaptic thalamocortical inputs, whereas longer-latency components increasingly reflect intracortical polysynaptic activity (Cruikshank et al. 2002; Happel et al. 2010; Intskirveli and Metherate 2012; Kawai et al. 2011). We measured the current sink's initial amplitude (first 5 ms from onset) and peak amplitude (over 20–50 ms from response

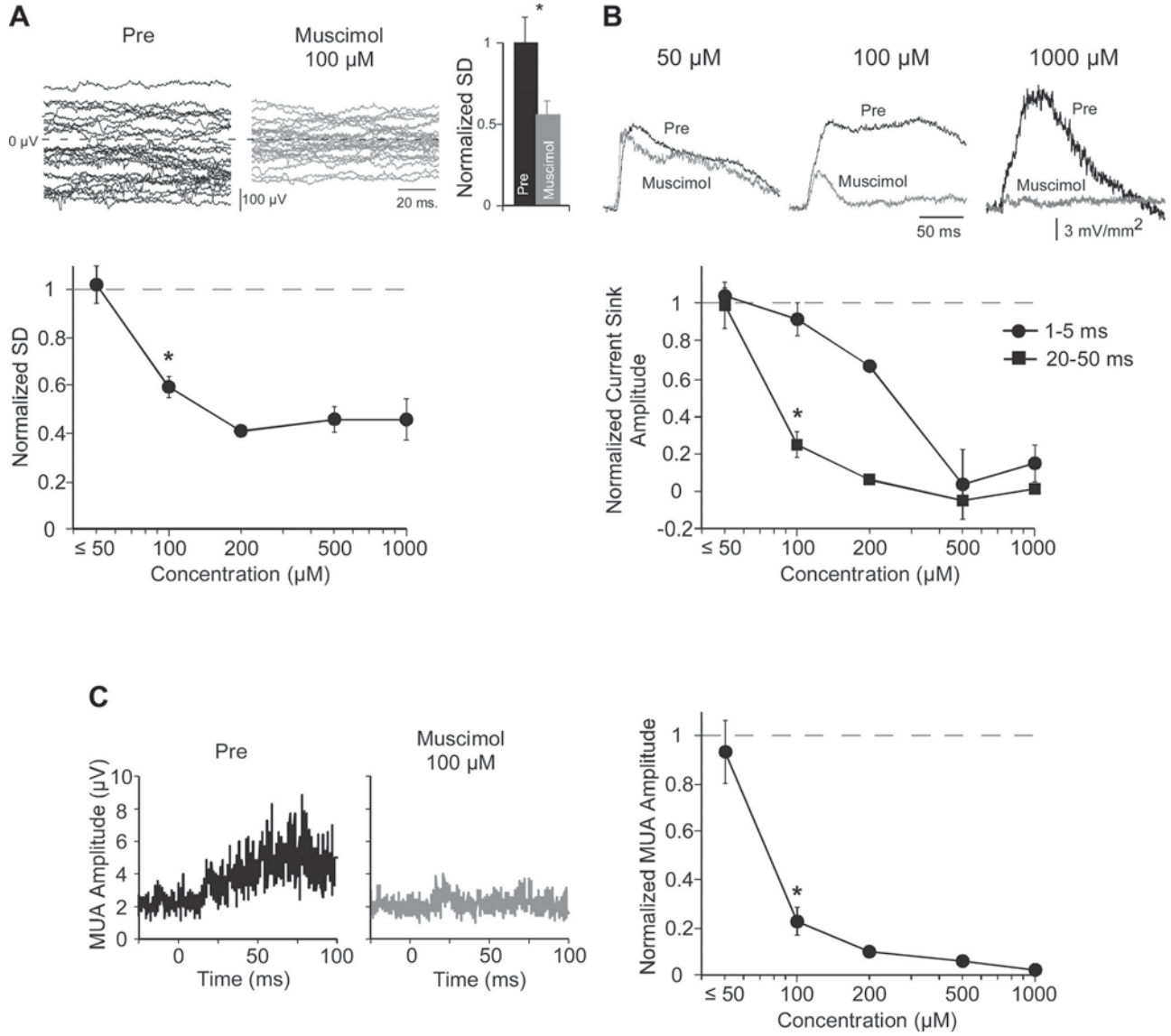

Fig. 2. Dose-dependent effects of muscimol on afferent vs. intracortical responses in layer 4 demonstrate selective inhibition of latter with optimal dose (100 μM). *A*: muscimol (100 μM) inhibited spontaneous LFP fluctuations in example traces from predrug and muscimol conditions (*top*, *left* and *center*). Fluctuations were quantified as the SD of the mean LFP for twenty-five 100-ms prestimulus epochs, normalized to predrug values and averaged across animals (histogram, *top right*; $n = 9$). A similar analysis at each dose (graph, *bottom*) showed no effect for ≤50 μM and reduced fluctuations at 100 μM (*; see RESULTS). *B*: effects of muscimol on CF-evoked current sinks are shown in example traces (*top*) and group data (*bottom*) and reveal a differential effect at 100 μM on initial (first 5 ms from onset) and peak (20–50 ms from onset) current sinks, each normalized to predrug values. *C*: effect of muscimol on CF-evoked multiunit activity (MUA). Example of average rectified MUA (*left*; tone onset at 0 ms) and group data (*right*; normalized to predrug MUA amplitude) show significant reduction of MUA by 100 μM muscimol.

onset) to assess thalamocortical and intracortical activity, respectively. The effects of muscimol on the layer 4 current sink are shown in Fig. 2*B* (examples, *top*; group data, *bottom*). Muscimol at the lowest concentrations (10–50 μM, $n = 4$) had little effect on either the initial amplitude (normalized amplitude 1.04 ± 0.045 of predrug value) or peak amplitude (0.99 ± 0.123 of predrug value), whereas at the highest doses (500-1,000 μM, $n = 4$) the drug reduced both initial and peak amplitudes almost completely (initial amplitude 0.09 ± 0.091 of predrug value, peak amplitude −0.02 ± 0.019 of predrug value). However, at an intermediate dose of 100 μM muscimol had no effect on the initial response (0.914 ± 0.089 of predrug, $n = 9$, paired *t*-test, $P > 0.05$) but significantly reduced peak amplitude (0.25 ± 0.074, $P < 0.001$; Fig. 2*B*, *top center* and *bottom*). Thus, at the 100 μM dose, muscimol differentially affected initial and peak responses, suggesting differential effects on thalamocortical and intracortical activity, respectively.

For a third, and most direct, measure of intracortical activity, we determined the effect of muscimol on acoustic-evoked MUA. MUA was extracted from single-trial, tone-evoked LFPs in layer 4 with a high-pass filter (>500 Hz), rectified, and averaged across 25 trials (O'Connell et al. 2011). An example of an average rectified response is in Fig. 2*C*, *left*, along with group data (Fig. 2*C*, *right*; each data point normalized to its predrug value). Muscimol at low doses of 10–50 μM had little effect on MUA (0.93 ± 0.128 of predrug value, paired *t*-test, $P > 0.05$, $n = 4$), whereas 100 μM muscimol reduced MUA nearly 80% (0.22 ± 0.059, $P < 0.001$, $n = 9$). Higher doses reduced MUA almost completely (500-1,000 μM combined: 0.04 ± 0.012, $P < 0.02$, $n = 4$). Muscimol at 100 μM and higher doses strongly reduced intracortical activity, as reflected in MUA.

Note the similarity of muscimol's dose-dependent reduction of three measures of intracortical activity: spontaneous LFP fluctuations (Fig. 2*A*), evoked current-sink peak (Fig. 2*B*), and evoked MUA (Fig. 2*C*). At the 100 μM dose, all presumed intracortical measures are strongly reduced, whereas there is little effect on the initial current-sink evoked response (Fig. 2*B*). The graphs in Fig. 2, *A–C*, indicate IC_{50} values that imply a similar mechanism of action on spontaneous LFP fluctuations (IC_{50} 86 μM), current sink over 20–50 ms (IC_{50} 91 μM), and evoked MUA (IC_{50} 82 μM) that differs from muscimol's effect on the initial current sink (IC_{50} 262 μM). We conclude that muscimol at a dose of 100 μM can inhibit intracortical activity without affecting thalamocortical inputs.

We also determined the effect of muscimol on CF threshold in layer 4, which in turn must depend on the threshold for activating thalamocortical inputs. Across all animals, predrug CF threshold averaged 8.0 ± 0.85 dB SPL ($n = 22$). Changes after muscimol were monitored by redetermining threshold in steps of 0 dB, 10 dB, and 20 dB above predrug value. At concentrations of 10–200 μM, muscimol had no effect on threshold (pre- and postmuscimol thresholds each averaged 7.5 ± 1.14 dB, $n = 14$). However, at 500-1,000 μM, thresholds increased at least 20 dB (predrug threshold 10.0 ± 0.0 dB SPL, $n = 4$; postmuscimol threshold was 30 dB in 2 animals, and 2 others had no response at 30 dB but did respond at higher, suprathreshold intensities). These threshold data suggest, again, that 100 μM muscimol does not reduce thalamocortical inputs.

Next, using the apparent optimal dose of 100 μM muscimol, we extended the analysis of CF-evoked responses to the current sinks in layers 2/3 and 5/6 and added controls for vehicle administration (Fig. 3, examples in *A*, group data in *B* and *C*; CF-evoked amplitudes normalized to peak response in "Pre" condition for each animal). In addition, for an independent measure of the drug's ability to affect all cortical layers, we measured spontaneous LFP fluctuations in each layer. Microapplication of vehicle (ACSF) to the A1 surface or intracortically (same parameters as for muscimol, above) had no effect on spontaneous LFP amplitude or on any amplitude or latency measure for evoked current sinks in any layer [Fig. 3*A*, *left*, and *B*; $n = 4$, pre-ACSF vs. post-ACSF paired *t*-tests, all *P* values > 0.05; normalized spontaneous SD: layer 2/3 1.00 ± 0.137 vs. 1.11 ± 0.173, layer 4 1.00 ± 0.102 vs. 1.07 ± 0.120, layer 5/6 1.00 ± 0.134 vs. 1.12 ± 0.149; onset latency (ms): layer 2/3 19.6 ± 2.80 vs. 20.8 ± 3.34, layer 4 14.9 ± 0.39 vs. 16.5 ± 0.27, layer 5/6 11.5 ± 0.43 vs. 12.9 ± 0.93; normalized initial amplitude: layer 2/3 0.43 ± 0.094 vs. 0.20 ± 0.048, layer 4 0.24 ± 0.039 vs. 0.21 ± 0.035, layer 5/6 0.17 ± 0.031 vs. 0.30 ± 0.066; normalized peak amplitude: layer 2/3 0.48 ± 0.115 vs. 0.48 ± 0.116, layer 4 0.73 ± 0.075 vs. 0.38 ± 0.081, layer 5/6 0.70 ± 0.056 vs. 0.51 ± 0.101].

In contrast to vehicle, 100 μM muscimol had dramatic yet selective effects on response parameters (Fig. 3*A*, *right*, and *C*). Muscimol strongly reduced spontaneous LFP fluctuations, similarly in each layer, demonstrating that its effects extended throughout the cortical depth (Fig. 3*C*, *left*; normalized SD, predrug vs. post-drug paired *t*-tests, $n = 9$: layer 2/3, 1.00 ± 0.197 vs. 0.576 ± 0.122, $P = 0.003$; layer 4, 1.00 ± 0.156 vs. 0.56 ± 0.075, $P = 0.003$; layer 5/6, 1.00 ± 0.155 vs. 0.64 ± 0.061, $P = 0.014$). For CF-evoked current sinks in each layer, muscimol did not affect the earliest response measures, i.e., both onset latency and initial amplitude were unaffected [Fig. 3*C*, *center* and *right*; $n = 7–9$, *P* values > 0.05; onset latency (ms): layer 2/3 20.6 ± 2.34 vs. 21.0 ± 1.92, layer 4 17.6 ± 1.02 vs. 18.5 ± 0.99, layer 5/6 12.6 ± 0.72 vs. 14.2 ± 0.84; normalized initial amplitude: layer 2/3 0.17 ± 0.038 vs. 0.12 ± 0.020, layer 4 0.23 ± 0.032 vs. 0.18 ± 0.025, layer 5/6 0.31 ± 0.036 vs. 0.36 ± 0.056]. However, as exemplified by the CSD profile in Fig. 3*A*, *right*, muscimol strongly reduced longer-latency components of the response (Fig. 3*C*, *right*). For the layer 2/3 and layer 4 current sinks peak amplitudes were reduced 80% or more, but, surprisingly, despite the small size of the layer 5/6 current sink, muscimol did not affect its peak amplitude ($n = 7–9$; normalized peak amplitude: layer 2/3, 0.81 ± 0.040 vs. 0.06 ± 0.036, $P < 0.001$; layer 4, 0.92 ± 0.021 vs. 0.21 ± 0.049, $P < 0.001$; layer 5/6, 0.69 ± 0.058 vs. 0.64 ± 0.081, $P > 0.05$).

Muscimol's lack of effect on the layer 5/6 current sink raises the question of whether the drug reached the deeper layers in effective concentrations. We addressed this issue in three ways. First, as noted above, muscimol reduced spontaneous LFP fluctuations ~50% in each layer, including layer 5/6 (Fig. 3*C*, *left*). Second, after initial experiments during which surface application of muscimol failed to affect the layer 5/6 current sink, in remaining experiments we microinjected muscimol directly into the middle layers at a depth of ~400 μm, i.e., at or below the layer 4 current sink and above the layer 5/6 sink. Neither delivery method reduced the layer 5/6 current sink [pre- vs. postdrug normalized peak amplitude, paired *t*-test, *P*

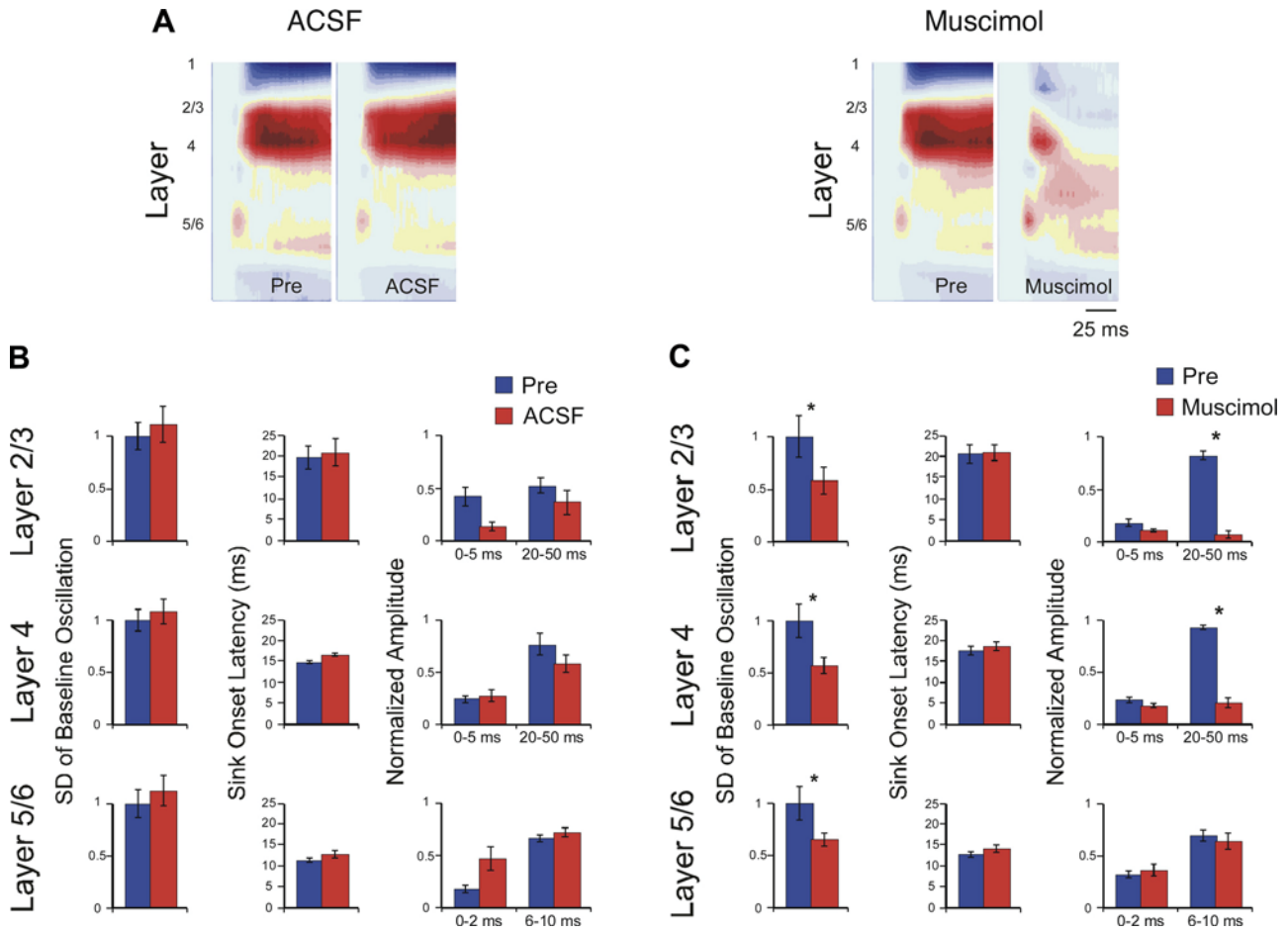

Fig. 3. Muscimol (100 μM) effects on thalamocortical vs. intracortical components of CF-evoked current sinks in layers 2/3, 4, and 5/6. *A*: example CSD profiles showing effects of control (ACSF, *left*) or muscimol (100 μM, *right*) microapplication; tone onset at beginning of plot, color scale as in Fig. 1. *B*: control injections had no effect on spontaneous fluctuations (*left*), current sink onset latencies (*center*), or response amplitudes (*right*; response amplitudes in *B* and *C* normalized to predrug peak values). *C*: muscimol reduced spontaneous fluctuations in all layers (*left*), had no effect on current sink onset latencies (*center*), and reduced peak response amplitudes in layers 2/3 and 4 but did not affect initial response amplitudes in any layer or peak amplitude in layer 5/6 (*right*).

values $>$ 0.05; surface muscimol (n = 3) 0.61 $\pm$ 0.104 vs. 0.78 $\pm$ 0.079, intracortical muscimol (n = 4) 0.76 $\pm$ 0.061 vs. 0.63 $\pm$ 0.081]. Third, in experiments using higher muscimol concentrations (500-1,000 μM) but identical drug volumes, the drug strongly reduced the deep-layer CF-evoked response in 2/4 cases (data not shown), similarly to its effect in layer 4 (Fig. 2*B*). That is, even though high muscimol concentrations preclude an interpretation of pre- vs. postsynaptic action, the drug's effect on the layer 5/6 response confirms penetration into deeper layers. Taken together, these three results indicate that the layer 5/6 current sink is not reduced by 100 μM muscimol and, therefore, likely does not contain an intracortical component (see also Fig. 4, *B* and *C*).

Laminar and spectral extent of thalamocortical inputs. Thus far, the results show that 100 μM muscimol appears to distinguish between thalamocortical inputs and intracortical responses in A1 by selectively inhibiting the latter. To determine the spectral breadth of thalamocortical inputs for the current sinks in layers 2/3, 4, and 5/6, we next extended the analysis to stimulus frequencies away from CF, up to 1 octave above CF and 2 octaves below, in quarter-octave steps. An example is in Fig. 4*A*, where tone-evoked CSD profiles are shown for a 2-octave range of stimuli. As expected, muscimol (100 μM) greatly reduced the amplitude of longer-latency responses to all stimulus frequencies. Notably, in layers 2/3 muscimol also eliminated short-latency responses to stimuli 0.5 octave or more below CF, and in layer 4 the drug eliminated short-latency responses to the most distant stimuli, 1.25 and 1.5 octaves below CF. In layer 5/6, however, muscimol did not reduce the response to any stimulus frequency.

To quantify these effects, for each current sink we measured RF breadth, i.e., the range of stimulus frequencies to which there was a response ($>3 \times$ SD above baseline, see MATERIALS AND METHODS), and averaged this value across animals, before and after muscimol. As shown in Fig. 4*B*, *top*, muscimol reduced RF breadth (from predrug to postdrug, n = 7–9, paired t-test): 42% in layer 2/3, from 2.4 $\pm$ 0.14 to 1.4 $\pm$ 0.11 octaves (P = 0.003); 14% in layer 4, from 2.2 $\pm$ 0.12 to 1.9 $\pm$ 0.10 octaves (P = 0.007); and not at all in layer 5/6 (1.8 $\pm$ 0.10 to 1.7 $\pm$ 0.12 octaves, $P > 0.05$). Given the concern noted above, that lack of drug effect in layer 5/6 might result from ineffective surface application, we repeated this analysis using only data from animals with intracortical muscimol microinjections. Still, we obtained the same result, shown in Fig. 4*B*, *bottom* (pre- vs. postdrug RF breadth, in octaves, paired t-test, n = 4; layer 2/3, 2.5 $\pm$ 0.10 vs. 1.6 $\pm$ 0.12, P = 0.009; layer 4, 2.4 $\pm$ 0.07 vs. 1.8 $\pm$ 0.12, P = 0.003; layer 5/6, 2.0 $\pm$ 0.18 vs. 1.8 $\pm$ 0.25, $P > 0.05$). Thus muscimol reduced RF breadth for

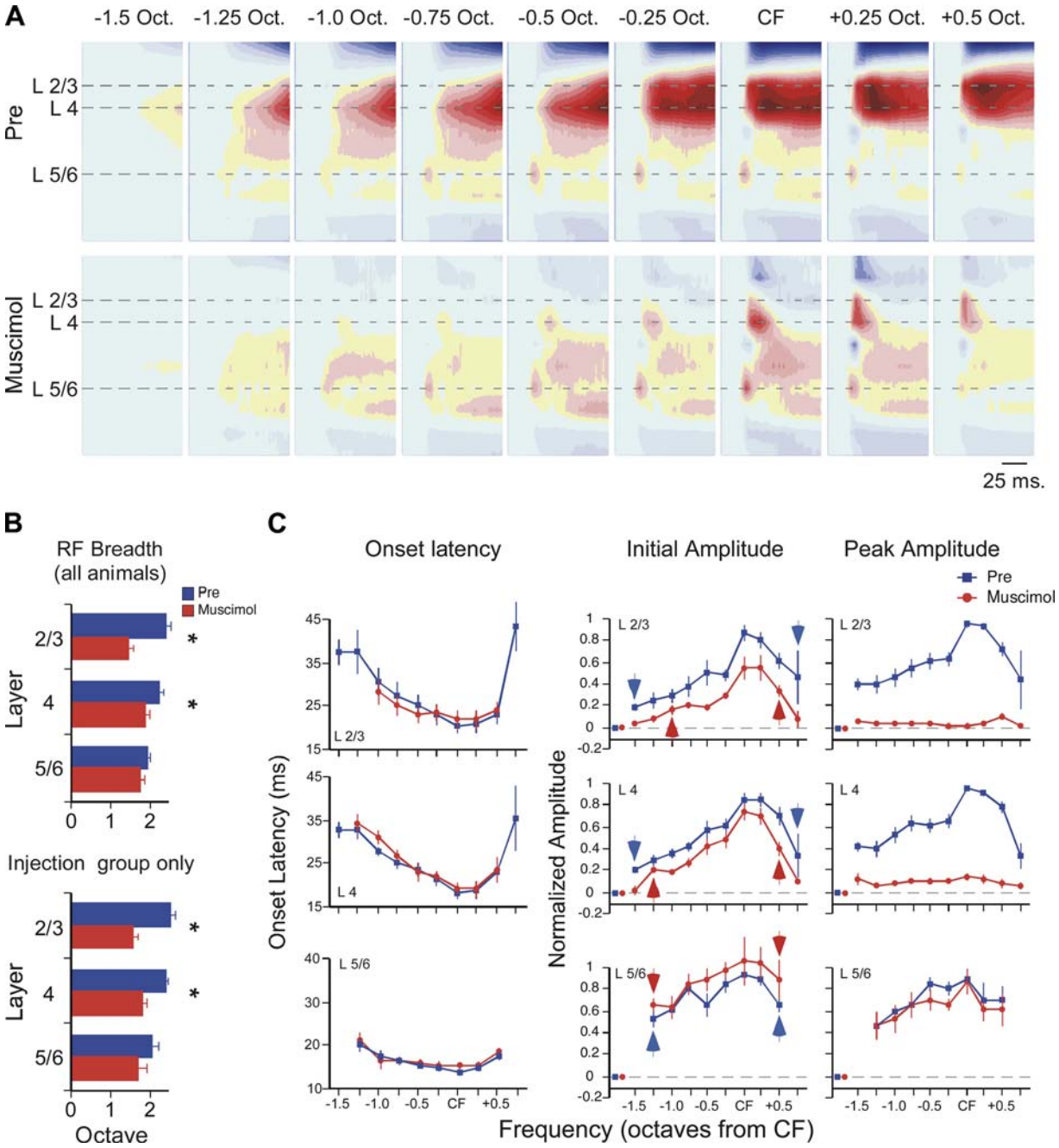

Fig. 4. Muscimol (100 μM) reveals the laminar and spectral extent of afferent inputs to primary auditory cortex (A1). *A*: example of muscimol effect on CSD profiles evoked by tone stimuli spanning 2 octaves (tone onset at beginning of plot for each CSD profile, color scale as in Fig. 1). *B*: across all animals (*top* histogram, $n = 7$–9), muscimol reduced receptive field (RF) breadth in layer 2/3 and layer 4 but not layer 5/6. Similar results were seen in the subset of experiments with intracortical microinjection of muscimol (i.e., excluding results from surface application; *bottom* histogram, $n = 4$). *C*: muscimol had no effect on current-sink onset latency for any tone-evoked response in any layer (*left*). For tone-evoked current sinks in muscimol, RF breadth based on initial amplitude (0–5 ms from onset) indicates breadth of presumed thalamocortical RF (red arrows, *center*). Similarly, blue arrows indicate edges of predrug mean RF (individual RF edges defined based on difference from prestimulus baseline; see MATERIALS AND METHODS). Muscimol-induced reduction of peak amplitude (20–50 ms from onset, *right*) indicates substantial intracortical contribution to RF in layers 2/3 and 4 but not layer 5/6. For stimulus-evoked responses, isolated red and blue data points near origin of each graph indicate mean value for prestimulus baseline (error bars are contained within symbol).

current sinks in the middle and upper layers but not in the deeper layers.

For stimulus-evoked responses that persisted in muscimol, we found no change in onset latency from predrug values (Fig. 4*C*, *left*; ANOVAs for each current sink, P values > 0.05). This lack of change in onset latency, despite significant reductions in peak amplitude (Fig. 4*C*, *right*), further indicates that muscimol-insensitive responses reflect monosynaptic afferent inputs. Note that for each current sink, onset latency increases with spectral distance from CF, as observed throughout the auditory system (e.g., see Kaur et al. 2004); however, it is noteworthy that this trend is more pronounced in layers 2/3 and 4 than in layer 5/6. Since onset responses likely reflect thalamocortical inputs, we therefore measured the spectral

breadth of muscimol-insensitive responses (initial amplitude, first 5 ms) to estimate the "thalamocortical RF," with group results in Fig. 4*C*, *center* (red graphs; all amplitudes normalized to peak "Pre" response, separately for each layer). The edges of the group RF in each layer were determined by comparing response amplitudes to prestimulus activity (prestimulus mean indicated on each graph by a single data point near the origin), beginning with the frequency most distant from CF and continuing toward CF until a statistically significant response was encountered (paired *t*-test); this response was considered the RF "edge" and is indicated Fig. 4*C*, *center*, by a red arrow (layer 2/3, baseline vs. response at −1.0 octave, paired *t*-test, $n = 7$, $P = 0.004$; layer 4, baseline vs. −1.25-octave response, $n = 9$, $P < 0.001$; layer 5/6, baseline vs. −1.25-octave response, $n = 9$, $P < 0.001$). For comparison, Fig. 4*C* also shows predrug RFs for each current sink with RF edges marked in the same way (blue graphs and arrows; note that only points within the predrug RF are shown, defined as in MATERIALS AND METHODS, to better visualize changes within the RF, and as a result some RF edges appear abrupt). (Predrug baseline means are not different from baseline means in muscimol, paired *t*-tests, *P* values > 0.05.) Finally, we also measured changes in peak amplitude (Fig. 4*C*, *right*). Muscimol strongly reduced peak amplitudes in layers 2/3 and 4 (ANOVAs for each current sink, *P* values < 0.001), demonstrating the presence of significant intracortical activity; however, muscimol again had no effect in layer 5/6 (ANOVA, $P > 0.05$). Consistent with the RF data in Fig. 4*B*, the data in Fig. 4*C* show that muscimol reduces the breadth and amplitude of current-sink RFs in layers 2/3 and 4 and can identify the "thalamocortical RF" in each layer. These thalamocortical inputs are amplified substantially in layers 2/3 and 4 by intracortical circuits; however, there is little amplification in layer 5/6.

To determine how thalamocortical and intracortical contributions evolve over the time course of each current sink, we measured the amplitude of predrug and muscimol-insensitive responses in 5-ms increments (2-ms increments in layer 5/6). Example traces from one animal are shown in Fig. 5*A*, and group data are in Fig. 5*B* (amplitudes normalized to peak predrug values, separately for each stimulus frequency and each layer). Muscimol-insensitive responses approximate the time course of thalamocortical monosynaptic potentials. Responses for which the first 5-ms interval does not differ from control (paired *t*-test, $P > 0.05$) are considered largely or entirely driven by thalamocortical inputs; in Fig. 5*B*, such responses are identified by dark gray background shading. For layers 2/3 and 4, even within this region of strong thalamocortical inputs, intracortical activity dominates the current sink within an additional few milliseconds, indicating rapid amplification of thalamic input by intracortical circuits. Outside of this central region of strong thalamocortical driving, muscimol

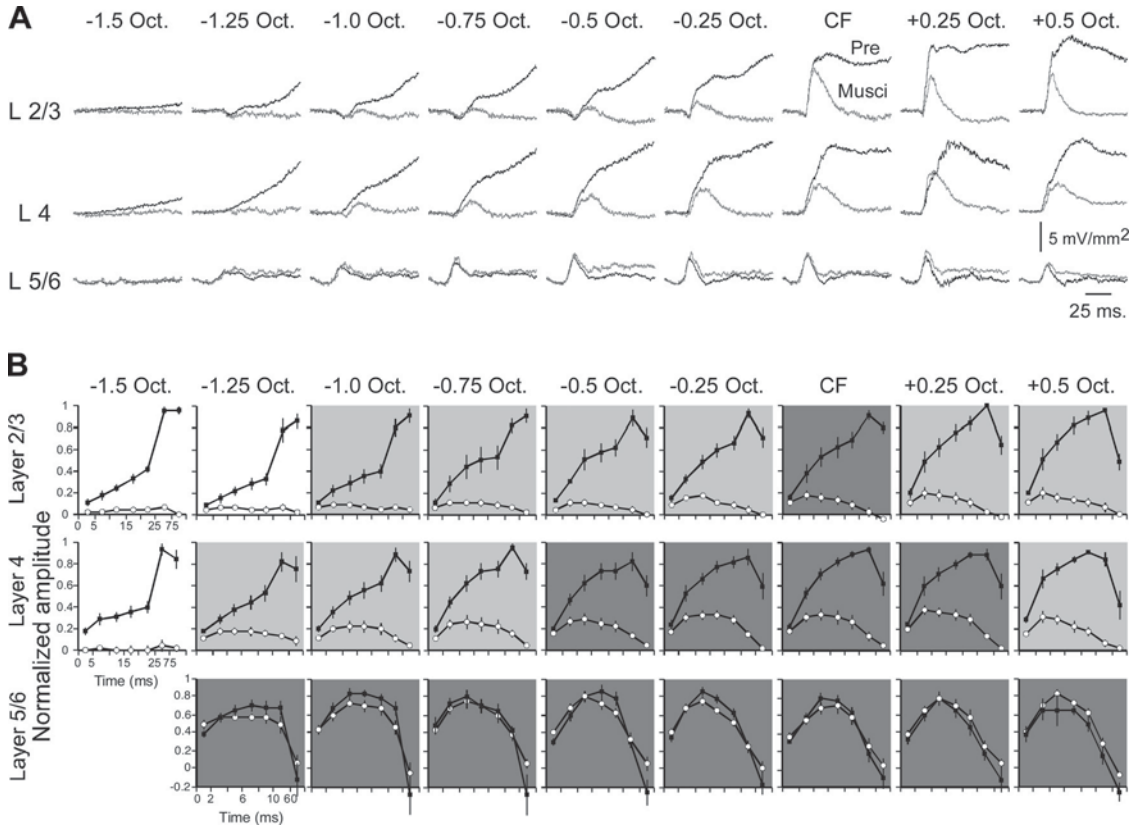

Fig. 5. Muscimol-insensitive responses reflect amplitude and time course of monosynaptic thalamocortical input. *A*: pre- and postmuscimol (100 μM) current sinks evoked by tone stimuli spanning 2 octaves. *B*: group data showing current sink amplitudes in 5-ms intervals for layer 2/3 (*top*) and layer 4 (*center*) and in 2-ms intervals for layer 5/6 (*bottom*) (■, predrug; ○, postmuscimol). Note that timescale is identical for *top* and *middle* (5-ms intervals up to last 2 data points, which are 25–75 ms and 75–300 ms intervals) and different for *bottom* (2-ms intervals up to last 2 data points, which are 10–60 ms and 60–300 ms intervals). For each graph, response amplitudes are normalized to predrug peak value. Dark gray shading indicates strongest thalamocortical input, where amplitude in first 5-ms interval is not reduced by muscimol; light gray shading indicates significant reduction in first 5 ms; and no shading indicates complete reduction of response by muscimol.

reduced response amplitudes even in the first 5-ms interval (paired *t*-test, $P < 0.05$), indicating significant intracortical activity; such responses are identified in Fig. 5*B* by light gray background shading. Finally, responses that were reduced completely by muscimol indicate complete dependence on intracortical ("horizontal") projections; these responses have no background shading in Fig. 5*B*.

In contrast to the rapid intracortical amplification of thalamic inputs in layers 2/3 and 4, the layer 5/6 current sink appears to depend solely on thalamocortical inputs throughout its time course and across its spectral RF, without any contribution from intracortical processing (Fig. 4*C*, *bottom*, and Fig. 5*B*, *bottom*). Note in Fig. 4*B*, *top*, that the average predrug RF in layer 5/6 (1.8 ± 0.10 octaves) is narrower than predrug RFs in layers 2/3 and 4 (vs. layer 2/3, 2.4 ± 0.14, $n = 7$, paired *t*-test, $P = 0.02$; vs. layer 4, 2.2 ± 0.12, $P = 0.04$), but this laminar difference in RF breadth disappears in muscimol (layer 5/6, 1.8 ± 0.12 octaves vs. layer 2/3, 1.4 ± 0.10, $P > 0.05$; vs. layer 4, 1.9 ± 0.10, $P > 0.05$). This result might be expected if intracortical circuits add breadth to thalamocortical RFs in layers 2/3 and 4 but not in layer 5/6. To our knowledge, the tone-evoked response in layer 5/6 has not previously been described as being solely thalamocortical in origin (see DISCUSSION).

DISCUSSION

The goal of this study was to reevaluate the use of muscimol in A1, and in doing so to identify thalamocortical and intracortical contributions to spectral integration. We first examined the effects of 10-1,000 μM muscimol and determined that an "optimal" 100 μM dose strongly reduced intracortical activity in layer 4—i.e., spontaneous LFP fluctuations, CF-evoked peak current sink, and MUA—without affecting measures of thalamocortical input—i.e., CF threshold and CF-evoked onset latency and initial amplitude. Thus muscimol at this dose appears to inhibit intracortical activity without reducing thalamocortical inputs. Using this optimal dose, we found that the breadth of muscimol-insensitive (presumed thalamocortical) RFs for the three major current sinks (in layers 2/3, 4, and 5/6) averaged 1.5–2 octaves (20 dB above CF threshold). A comparison to predrug RFs showed that in layers 2/3 and 4, intracortical circuits increase response amplitude manyfold and increase RF breadth by ~1 octave and ~0.3 octave, respectively, whereas in layer 5/6 intracortical circuits did not contribute at all to the RF (neither amplitude nor breadth). We conclude that in layer 5/6 the current-sink RF is wholly due to thalamocortical inputs, whereas in layers 2–4 intracortical circuits mediate rapid, local amplification of thalamic inputs and increase spectral integration via intracortical projections. Thus spectral integration within A1 is broader than the degree of integration evident in afferent inputs.

Interpretation of tone-evoked CSD profiles and RFs. Current sinks in the CSD profile are thought to reflect the location, timing, and magnitude of synaptic excitation underlying tone-evoked responses (Cruikshank et al. 2002; Happel et al. 2010; Intskirveli and Metherate 2012; Muller-Preuss and Mitzdorf 1984; Steinschneider et al. 1992). We focused on three current sinks that are the most reliable tone-evoked responses. The layer 4 current sink was easily identified in every experiment as the earliest sink in the middle layers and undoubtedly reflects the main input from the lemniscal auditory thalamus [ventral division of the medial geniculate body (MGv)] (Cruikshank et al. 2002). The layer 2/3 current sink is located 100 μm above the layer 4 sink, and its longer onset latency might suggest that it is at least one synapse beyond the thalamocortical input. However, the onset latency of the layer 2/3 sink was not affected by muscimol, which could indicate either non-primary afferent input (e.g., slower-conducting thalamocortical axons) or an intracortical response that requires a higher dose of muscimol to silence (e.g., an exceptionally secure disynaptic relay) (Cruikshank et al. 2007; Douglas and Martin 1991; Gil et al. 1999; Rose and Metherate 2005). Note that a recent study using optogenetic activation of thalamocortical terminals in A1 found activation of neurons in layer 2/3 (Ji et al. 2015), demonstrating direct thalamic input (either lemniscal or non-lemniscal) to some neurons. Finally, the layer 5/6 current sink is relatively small and brief, and its onset latency is earlier than that of the layer 4 sink. This deep-layer sink likely reflects collateral projections of the main thalamocortical projection to layer 4, as has been proposed in anatomical and physiological studies (Constantinople and Bruno 2013; Cruikshank et al. 2002; Zhou et al. 2010). Given that the change in onset latency with spectral distance from CF is substantially less in layer 5/6 than in more superficial layers (Fig. 4*C*, *left*), we speculate that thalamocortical inputs are still myelinated at this point, which could increase conduction velocity ~10-fold (Salami et al. 2003). Finally, the insensitivity of the layer 5/6 sink to muscimol is consistent with findings that sensory-evoked responses in layer 5/6 of visual or somatosensory cortex reflect direct thalamic inputs and are little, if at all, influenced by more superficial layers (Constantinople and Bruno 2013; Schwark et al. 1986).

Since current sinks largely reflect synaptic potentials in neurons near the multiprobe, a current-sink RF is the range of stimulus frequencies that drives local synapses, and as such is a measure of spectral integration within a local cortical region. Importantly, the current-sink RF includes stimulus frequencies that elicit subthreshold inputs as well as the narrower range that elicits postsynaptic spikes (the conventional RF measure). As expected, therefore, RFs in the present study tend to be broader than RFs based on spikes, as are RFs in previous studies using intracellular recordings, LFPs, and CSD profiles (Calford et al. 1983; Galvan et al. 2002; Happel et al. 2010; Kaur et al. 2004; Linden et al. 2003; Norena and Eggermont 2002; Tan et al. 2004; Wehr and Zador 2003). For this study, intended to examine all spectral (including subthreshold) integration, the current-sink RF is an ideal measure.

Use of muscimol to probe function in A1. As noted in the introduction to this article, muscimol has been used in A1 mostly for two reasons: to reversibly inactivate A1 (without affecting passing axons) or to silence cortical neurons so that any remaining evoked activity can be attributed to afferent inputs. The former usage typically involves a dose of 5–20 mM, or even higher (up to 75 mM) when the drug is expected to act chronically or at a distance (Jaramillo and Zador 2011; Smith et al. 2004; Talwar et al. 2001), and the use of muscimol for this purpose in A1 and other brain regions is widely accepted (Allen et al. 2008; Edeline et al. 2002; Martin and Ghez 1999; Reiter and Stryker 1988). The second use of muscimol—to isolate afferent responses—requires a carefully chosen dose that should reduce afferent EPSPs enough to

prevent action potentials yet not so much as to preclude observation of the synaptic response itself (e.g., due to excessive postsynaptic shunting). Importantly, it is assumed that neurotransmitter release from afferent inputs is not affected, since muscimol is a GABA-A receptor agonist and presynaptic GABA receptors typically are GABA-B receptors. However, a study of the calyx synapse in the brain stem suggests that muscimol may act at presynaptic GABA-B receptors (Yamauchi et al. 2000). Although a similar study showed no effect of muscimol on presynaptic GABA-B receptors in motor neurons (Delgado-Lezama et al. 2004), it is possible that muscimol might act at some GABA-B receptor subtypes but not others. Our results show that at a 100 μM dose muscimol apparently does not affect monosynaptic inputs to A1. That is, either the afferents do not express presynaptic GABA-B receptors or the receptors are not sensitive to muscimol at this dose. Note that even prior studies using higher (5 mM) muscimol doses found no difference between the effects of muscimol alone vs. its effects when paired with a drug intended to block any action at GABA-B receptors (Happel et al. 2014, 2010). Similarly, intracortical blockade of GABA-B receptors had no effect on the ability of neurons in rat A1 to follow trains of acoustic stimuli, i.e., no evidence for forward suppression mediated by GABA-B receptors (Yao et al. 2015). Nonetheless, our results do not address the question of whether muscimol at higher doses affects presynaptic receptors in A1, an issue that future experiments will need to resolve. Although muscimol at higher doses did reduce the afferent response (Fig. 2*B*), this likely involves, at least in part, its expected postsynaptic action at GABA-A receptors (postsynaptic shunting).

Our finding that 100 μM muscimol does not affect the first few milliseconds of the layer 4 current sink, even as it strongly reduces spontaneous LFP fluctuations, longer-latency evoked responses, and MUA, is consistent with prior results showing that the first few milliseconds of the tone-evoked layer 4 current sink reflects monosynaptic thalamocortical input (Cruikshank et al. 2002; Intskirveli and Metherate 2012; Metherate et al. 2012; Rose and Metherate 2005) as well as in vitro studies showing that 100 μM muscimol elicits strong inhibitory (postsynaptic) currents in cortical pyramidal neurons (Salgado et al. 2012). Overall, the results clearly suggest that our approach can separate thalamocortical and intracortical contributions to tone-evoked responses in A1.

Spectral breadth of thalamocortical and intracortical inputs. Using the optimal dose of muscimol, the present study provides estimates of the spectral breadth of thalamocortical inputs to three layers in A1 (Fig. 4*B*): in layer 4, inputs span an average range of 1.9 octaves around CF (20 dB above CF threshold), which increased 16% to 2.2 octaves as a result of intracortical processing; in layer 2/3, the input range of 1.4 octaves increased 71% to 2.4 octaves as a result of intracortical processing; and in layer 5/6, the input range of 1.7 octaves was not increased within the cortex. For all stimulus frequencies, intracortical processing rapidly amplified the response magnitude manyfold in layers 2/3 and 4 but not at all in layer 5/6. This intracortical amplification may underlie features of acoustic processing that depend on recurrent amplification in superficial and middle, but not deep, layers of A1 (Christianson et al. 2011). The increased RF breadth in layers 2/3 and 4 likely involves intracortical "horizontal" pathways, i.e., RF-edge frequencies depend on projections to the recording site from distant cortical regions where those frequencies are CF (Happel et al. 2010; Kaur et al. 2004). It is notable that neurons in layer 4 receive horizontal inputs from throughout much of the rostrocaudal extent of A1 (Kratz and Manis 2015). Importantly, this intracortical contribution to RF breadth demonstrates that spectral integration within A1 is broader than that found in auditory thalamic (and other subcortical) nuclei or, at least, broader than that relayed in thalamocortical afferents (Happel et al. 2010; Kadia and Wang 2003; Metherate 2011a). The main features of spectral integration demonstrated in this study are illustrated as a simple schematic in Fig. 6.

These estimates of the spectral breath of thalamocortical inputs resemble some results of previous studies that used muscimol doses an order of magnitude higher, despite methodological and species differences, although higher doses likely produced the larger effects of previous studies. In rat A1, intracortical injection of 5 mM muscimol reduced RF breadth in layer 4 from ~2.4 to <0.5 octaves (LFP and intracellular recordings, stimuli 20 dB above CF threshold) (Kaur et al. 2004). Similarly, with stimuli 60 dB above threshold, 1 mM muscimol reduced RFs from 3.4 to 1.2 octaves (intracellular recordings in rat A1) (Liu et al. 2007). In gerbil A1, surface application of 5 mM muscimol reduced RF breadth in layer 4 from 6.4 to 3.2 octaves (CSD recordings, 20 dB above threshold) (Happel et al. 2010). While direct comparisons are difficult because of technical differences, the present and prior results are qualitatively similar, with the lesser effects of muscimol in the present study likely due to use of a calibrated (lower) dose. However, our results are not consistent with the notion that RF breadth reflects only the spectral breadth of afferent input (Liu et al. 2007). Overall, the results support the conclusion of previous studies that spectral integration within A1 is uniquely broad because of intracortical integration (Happel et al. 2010; Kaur et al. 2004).

A surprising finding is that the layer 5/6 sink was insensitive to muscimol (100 μM), suggesting that it entirely reflects

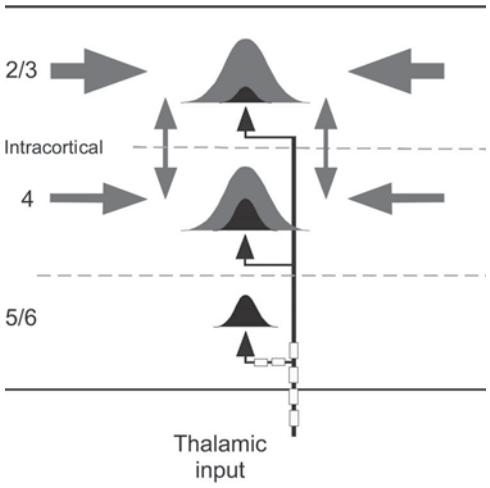

Fig. 6. Cartoon schematic depicting spectral integration in A1, based on present results. Gaussians represent RFs in layers 2/3, 4, and 5/6 with subfields determined by thalamocortical (black) and intracortical (gray) synapses. Thalamic inputs (black arrows) mediating CF and near-CF responses enter the cortex via myelinated axons and may retain myelination through the deep layers. Intracortical horizontal projections (gray arrows) from regions with higher or lower CFs contribute to spectral integration in layers 2/3 and 4 but not layer 5/6. Similarly, local connections (vertical double arrows) amplify responses in layers 2/3 and 4 but not 5/6.

afferent inputs and not intracortical circuits. Previous findings that the deep-layer current sink was sometimes reduced by muscimol may reflect the use of doses >1 mM (indeed, in our experiments higher doses also could reduce the layer 5/6 response), but overall previous results are generally consistent with a strong thalamocortical contribution (Cruikshank et al. 2002; Happel et al. 2010; Zhou et al. 2010). However, intracellular recordings show that the thalamocortical inputs to layer 5/6 can activate inhibition (Zhou et al. 2010), which indicates activation of cortical circuits. Thus the lack of an intracortical contribution in our study may result, in part, from methodology (e.g., level and type of anesthesia), and intracortical activity may be evoked more readily in other conditions, such as during behavior. Nonetheless, the results provide an estimate of the spectral range of thalamocortical inputs to layer 5/6 and show that it is nearly identical to the range for superficial- and middle-layer inputs.

Taken together, the results of the present study show that muscimol can be used effectively to silence cortical neurons while affecting afferent inputs minimally, thereby allowing estimates of the spectral breadth and laminar distribution of thalamocortical inputs to A1. The results support the hypothesis that spectral integration in A1 is remarkably and uniquely broad, a feature that likely plays an important role in auditory cortical modulation and plasticity (Happel et al. 2010; Metherate 2011a).

ACKNOWLEDGMENTS

We thank Caitlin Askew for comments on the manuscript.

Present address of B. J. Vizcarra-Chacón: Dept. of Pharmacobiology, Centro de Investigación y de Estudios Avanzados del Instituto Politécnico Nacional, Mexico City 14330, Mexico.

GRANTS

This research was supported by grants from the National Institute on Deafness and Other Communication Disorders (R01 DC-013200 and P30 DC-08369) and fellowships from the National Council for Science and Technology (Mexico) and the Center for the Neurobiology of Learning and Memory (University of California, Irvine).

DISCLOSURES

No conflicts of interest, financial or otherwise, are declared by the author(s).

AUTHOR CONTRIBUTIONS

Author contributions: I.I., B.J.V.-C., and R.M. conception and design of research; I.I., A.J., and B.J.V.-C. performed experiments; I.I., A.J., B.J.V.-C., and R.M. analyzed data; I.I., B.J.V.-C., and R.M. interpreted results of experiments; I.I. prepared figures; I.I. and R.M. drafted manuscript; I.I. and R.M. edited and revised manuscript; I.I. and R.M. approved final version of manuscript.

REFERENCES

Allen TA, Narayanan NS, Kholodar-Smith DB, Zhao Y, Laubach M, Brown TH. Imaging the spread of reversible brain inactivations using fluorescent muscimol. *J Neurosci Methods* 171: 30–38, 2008.

Calford MB, Webster WR, Semple MM. Measurement of frequency selectivity of single neurons in the central auditory pathway. *Hear Res* 11: 395–401, 1983.

Christianson GB, Sahani M, Linden JF. Depth-dependent temporal response properties in core auditory cortex. *J Neurosci* 31: 12837–12848, 2011.

Constantinople CM, Bruno RM. Deep cortical layers are activated directly by thalamus. *Science* 340: 1591–1594, 2013.

Cruikshank SJ, Lewis TJ, Connors BW. Synaptic basis for intense thalamocortical activation of feedforward inhibitory cells in neocortex. *Nat Neurosci* 10: 462–468, 2007.

Cruikshank SJ, Rose HJ, Metherate R. Auditory thalamocortical synaptic transmission in vitro. *J Neurophysiol* 87: 361–384, 2002.

Delgado-Lezama R, Aguilar J, Cueva-Rolon R. Synaptic strength between motoneurons and terminals of the dorsolateral funiculus is regulated by GABA receptors in the turtle spinal cord. *J Neurophysiol* 91: 40–47, 2004.

Douglas RJ, Martin KA. A functional microcircuit for cat visual cortex. *J Physiol* 440: 735–769, 1991.

Edeline JM, Hars B, Hennevin E, Cotillon N. Muscimol diffusion after intracerebral microinjections: a reevaluation based on electrophysiological and autoradiographic quantifications. *Neurobiol Learn Mem* 78: 100–124, 2002.

Fritz J, Shamma S, Elhilali M, Klein D. Rapid task-related plasticity of spectrotemporal receptive fields in primary auditory cortex. *Nat Neurosci* 6: 1216–1223, 2003.

Froemke RC, Merzenich MM, Schreiner CE. A synaptic memory trace for cortical receptive field plasticity. *Nature* 450: 425–429, 2007.

Galvan VV, Chen J, Weinberger NM. Differential thresholds of local field potentials and unit discharges in rat auditory cortex. *Hear Res* 167: 57–60, 2002.

Gil Z, Connors BW, Amitai Y. Efficacy of thalamocortical and intracortical synaptic connections: quanta, innervation, and reliability. *Neuron* 23: 385–397, 1999.

Hackett TA, Barkat TR, O'Brien BM, Hensch TK, Polley DB. Linking topography to tonotopy in the mouse auditory thalamocortical circuit. *J Neurosci* 31: 2983–2995, 2011.

Happel MF, Deliano M, Handschuh J, Ohl FW. Dopamine-modulated recurrent corticoefferent feedback in primary sensory cortex promotes detection of behaviorally relevant stimuli. *J Neurosci* 34: 1234–1247, 2014.

Happel MF, Jeschke M, Ohl FW. Spectral integration in primary auditory cortex attributable to temporally precise convergence of thalamocortical and intracortical input. *J Neurosci* 30: 11114–11127, 2010.

Hogsden JL, Rosen LG, Dringenberg HC. Pharmacological and deprivation-induced reinstatement of juvenile-like long-term potentiation in the primary auditory cortex of adult rats. *Neuroscience* 186: 208–219, 2011.

Intskirveli I, Metherate R. Nicotinic neuromodulation in auditory cortex requires MAPK activation in thalamocortical and intracortical circuits. *J Neurophysiol* 107: 2782–2793, 2012.

Jaramillo S, Zador AM. The auditory cortex mediates the perceptual effects of acoustic temporal expectation. *Nat Neurosci* 14: 246–251, 2011.

Ji XY, Zingg B, Mesik L, Xiao Z, Zhang LI, Tao HW. Thalamocortical innervation pattern in mouse auditory and visual cortex: laminar and cell-type specificity. *Cereb Cortex* (May 15, 2015). doi: 10.1093/cercor/bhv099.

Kadia SC, Wang X. Spectral integration in A1 of awake primates: neurons with single- and multipeaked tuning characteristics. *J Neurophysiol* 89: 1603–1622, 2003.

Kaur S, Lazar R, Metherate R. Intracortical pathways determine breadth of subthreshold frequency receptive fields in primary auditory cortex. *J Neurophysiol* 91: 2551–2567, 2004.

Kawai HD, Kang HA, Metherate R. Heightened nicotinic regulation of auditory cortex during adolescence. *J Neurosci* 31: 14367–14377, 2011.

Kratz MB, Manis PB. Spatial organization of excitatory synaptic inputs to layer 4 neurons in mouse primary auditory cortex. *Front Neural Circuits* 9: 17, 2015.

Linden JF, Liu RC, Sahani M, Schreiner CE, Merzenich MM. Spectrotemporal structure of receptive fields in areas AI and AAF of mouse auditory cortex. *J Neurophysiol* 90: 2660–2675, 2003.

Liu BH, Wu GK, Arbuckle R, Tao HW, Zhang LI. Defining cortical frequency tuning with recurrent excitatory circuitry. *Nat Neurosci* 10: 1594–1600, 2007.

Martin JH, Ghez C. Pharmacological inactivation in the analysis of the central control of movement. *J Neurosci Methods* 86: 145–159, 1999.

Metherate R. Functional connectivity and cholinergic modulation in auditory cortex. *Neurosci Biobehav Rev* 35: 2058–2063, 2011a.

Metherate R. Modulatory mechanisms for controlling auditory processing. In: *Synaptic Mechanisms in the Auditory System*, edited by Trussell LO, Popper AN, Fay RR. New York: Springer, 2011b, p. 187–202.

Metherate R, Cox CL, Ashe JH. Cellular bases of neocortical activation: modulation of neural oscillations by the nucleus basalis and endogenous acetylcholine. *J Neurosci* 12: 4701–4711, 1992.

Metherate R, Intskirveli I, Kawai HD. Nicotinic filtering of sensory processing in auditory cortex. *Front Behav Neurosci* 6: 44, 2012.

Miller LM, Escabi MA, Read HL, Schreiner CE. Functional convergence of response properties in the auditory thalamocortical system. *Neuron* 32: 151–160, 2001.

Muller-Preuss P, Mitzdorf U. Functional anatomy of the inferior colliculus and the auditory cortex: current source density analyses of click-evoked potentials. *Hear Res* 16: 133–142, 1984.

Norena A, Eggermont JJ. Comparison between local field potentials and unit cluster activity in primary auditory cortex and anterior auditory field in the cat. *Hear Res* 166: 202–213, 2002.

O'Connell MN, Falchier A, McGinnis T, Schroeder CE, Lakatos P. Dual mechanism of neuronal ensemble inhibition in primary auditory cortex. *Neuron* 69: 805–817, 2011.

Palombi PS, Caspary DM. $GABA_A$ receptor antagonist bicuculline alters response properties of posteroventral cochlear nucleus neurons. *J Neurophysiol* 67: 738–746, 1992.

Palombi PS, Caspary DM. GABA inputs control discharge rate primarily within frequency receptive fields of inferior colliculus neurons. *J Neurophysiol* 75: 2211–2219, 1996.

Reiter HO, Stryker MP. Neural plasticity without postsynaptic action potentials: less-active inputs become dominant when kitten visual cortical cells are pharmacologically inhibited. *Proc Natl Acad Sci USA* 85: 3623–3627, 1988.

Romanski LM, LeDoux JE. Organization of rodent auditory cortex: anterograde transport of PHA-L from MGv to temporal neocortex. *Cereb Cortex* 3: 499–514, 1993.

Rose HJ, Metherate R. Auditory thalamocortical transmission is reliable and temporally precise. *J Neurophysiol* 94: 2019–2030, 2005.

Salami M, Itami C, Tsumoto T, Kimura F. Change of conduction velocity by regional myelination yields constant latency irrespective of distance between thalamus and cortex. *Proc Natl Acad Sci USA* 100: 6174–6179, 2003.

Salgado H, Garcia-Oscos F, Martinolich L, Hall S, Restom R, Tseng KY, Atzori M. Pre- and postsynaptic effects of norepinephrine on gamma-aminobutyric acid-mediated synaptic transmission in layer 2/3 of the rat auditory cortex. *Synapse* 66: 20–28, 2012.

Schwark HD, Malpeli JG, Weyand TG, Lee C. Cat area 17. II. Response properties of infragranular layer neurons in the absence of supragranular layer activity. *J Neurophysiol* 56: 1074–1087, 1986.

Smith AL, Parsons CH, Lanyon RG, Bizley JK, Akerman CJ, Baker GE, Dempster AC, Thompson ID, King AJ. An investigation of the role of auditory cortex in sound localization using muscimol-releasing Elvax. *Eur J Neurosci* 19: 3059–3072, 2004.

Steinschneider M, Tenke CE, Schroeder CE, Javitt DC, Simpson GV, Arezzo JC, Vaughan HG Jr. Cellular generators of the cortical auditory evoked potential initial component. *Electroencephalogr Clin Neurophysiol* 84: 196–200, 1992.

Steriade M, McCormick DA, Sejnowski TJ. Thalamocortical oscillations in the sleeping and aroused brain. *Science* 262: 679–685, 1993.

Stiebler I, Neulist R, Fichtel I, Ehret G. The auditory cortex of the house mouse: left-right differences, tonotopic organization and quantitative analysis of frequency representation. *J Comp Physiol* 181: 559–571, 1997.

Talwar SK, Musial PG, Gerstein GL. Role of mammalian auditory cortex in the perception of elementary sound properties. *J Neurophysiol* 85: 2350–2358, 2001.

Tan AY, Zhang LI, Merzenich MM, Schreiner CE. Tone-evoked excitatory and inhibitory synaptic conductances of primary auditory cortex neurons. *J Neurophysiol* 92: 630–643, 2004.

Wang J, Caspary D, Salvi RJ. GABA-A antagonist causes dramatic expansion of tuning in primary auditory cortex. *Neuroreport* 11: 1137–1140, 2000.

Wehr M, Zador AM. Balanced inhibition underlies tuning and sharpens spike timing in auditory cortex. *Nature* 426: 442–446, 2003.

Weinberger NM. Specific long-term memory traces in primary auditory cortex. *Nat Rev Neurosci* 5: 279–290, 2004.

Winer JA, Miller LM, Lee CC, Schreiner CE. Auditory thalamocortical transformation: structure and function. *Trends Neurosci* 28: 255–263, 2005.

Yamauchi T, Hori T, Takahashi T. Presynaptic inhibition by muscimol through $GABA_B$ receptors. *Eur J Neurosci* 12: 3433–3436, 2000.

Yao JD, Bremen P, Middlebrooks JC. Emergence of spatial stream segregation in the ascending auditory pathway. *J Neurosci* 35: 16199–16212, 2015.

Zhou Y, Liu BH, Wu GK, Kim YJ, Xiao Z, Tao HW, Zhang LI. Preceding inhibition silences layer 6 neurons in auditory cortex. *Neuron* 65: 706–717, 2010.